

Fig. 3 Predicted final range R_p vs updating time t_1 for noncoplanar problem with various nonoptimal evader thrust angles α_{1e} and α_{2e} .

updating method in real-time, however, does not appear feasible because of the large number of equations that must be integrated between updates.

The basic noncoplanar problem has the same rocket thrust and I_{sp} as the coplanar problem, but with initial mass $m(0) = 1250$ slugs (18,237.5 kg) for both vehicles. The evader's initial conditions are the same, whereas the pursuer's initial conditions are

$$\begin{aligned} r_p &= 1.02 & V_{r_p} &= 0.46 & \phi_p &= 1.23 \\ V_{\phi_p} &= -0.35 & \theta_p &= 1.5 & V_{\theta_p} &= 0.38 \end{aligned} \quad (8)$$

The final range with optimal play by both vehicles is 16.73 naut miles (30.45 km).

Figure 3 shows the predicted final range R_p as a function of updating time t_1 for a number of sets of nonoptimal evader thrust angles. An updating interval of $\Delta t = 0.024$ TU with the matrix Riccati updating method was used in all cases. This R_p tends to oscillate more than in the coplanar problems, especially at the start of the problem, where R_p generally decreases at the first update, increases at the second, after which it slowly decreases. This difficulty at the second update is probably due to instability in the integration of the matrix Riccati equation.

As for possible real-time implementation of this method for noncoplanar problems (with state vector having dimension 12), the maximum computation time required between updates is about 32 sec, compared to an actual updating interval of 19.4 sec ($\Delta t = 0.024$ TU). As with the coplanar problem, efficient programming and use of the symmetry of the S matrix should allow real-time implementation.

Conclusions

The principal conclusion is that the near optimal feedback control law allows the pursuing spacecraft to take advantage of nonoptimal play of the evader to reduce the final range. With efficient programming, this technique probably can be implemented in real time, using the matrix Riccati updating technique.

However, this technique is not as effective when the predicted final range approaches zero, when nonunique controls occur. One possible solution to this problem is to use the near optimal control law until the predicted final range reaches some specified small value, and then to switch to some other guidance technique, such as proportional navigation.

The instability of the numerical backward integration of the matrix Riccati differential equation is another problem area, especially with the noncoplanar problems. The integration technique used in the simulations was a four point Adams-Bashforth-Moulton predictor-corrector routine that is started

by a fifth-order Runge-Kutta method. It is possible that other numerical integration techniques would result in greater stability.

Another problem with this technique is that a solution to the initial TPBVP is required to start the method. Numerically solving a TPBVP is too time consuming to be a viable solution. It may be possible, however, to store the initial costates associated with a number of expected initial states. The method then could be started, either by using the costate vector from the solution closest to the actual initial state, or by interpolating to get an improved estimate of the optimal costate vector.

References

- Anderson, G. M., "A Near Optimal Closed-Loop Solution Method for Non-Singular Zero-Sum Differential Games," *Journal of Optimization Theory and Applications*, Vol. 13, March 1974, pp. 303-318.
- Anderson, G. M., "A Transition Matrix Method for Generating Near Optimal Closed-Loop Solutions to Nonlinear Zero-Sum Differential Games," *International Journal of System Sciences*, Vol. 7, May 1976, pp. 529-543.
- Bryson, A. E. and Ho, Y. C., *Applied Optimal Control*, Ginn and Company, Waltham, Mass., 1969.

A Computationally Fast One-Dimensional Diffusion-Photochemistry Model of SST Wakes

Gregory L. Matloff* and Martin I. Hoffert†
New York University, New York, N. Y.

Introduction

SENSITIVITY studies of models describing global effects of perturbations to the stratospheric ozone layer caused by large-scale operations of aerospace vehicles require consideration of wake photochemistry and diffusion. A computational method applicable to such analysis in the early postvortex phase is presented in this Note. Because of the computational rapidity of the method, sensitivity studies of SST effluent effects upon ozone depletion can be readily accomplished. Comparison with other studies and predictions of some characteristics for global NO_x input are provided.

Derivation and Chemistry

Consider a turbulent plume of cross-sectional area A , which grows with increasing distance x from the origin by turbulent entrainment of material from the surrounding free stratosphere. The conservation of species i mass equation is¹

$$d(\rho_i \bar{U} A) / dx = d(\rho_{ie} \bar{U} A) / dx + A \rho_i \quad (1)$$

where ρ_i is the area-averaged partial mass density within wake, ρ_{ie} is the constant edge (or ambient) partial density, \bar{U} is the (constant) wind velocity or airspeed in a vehicle-fixed coordinate system, and $\dot{\rho}_i$ is the creation or destruction of species i (mass/volume/time) by chemical transformation. The left-hand side of Eq. (1) represents the rate of change of

Received Jan. 10, 1977; revision received April 20, 1977.

Index categories: Thermochemistry and Chemical Kinetics; Air-breathing Propulsion; Environmental Effects.

*Research Scientist, Department of Applied Science. Member AIAA.

†Associate Professor, Department of Applied Science. Member AIAA.

species i (mass/time/plume length) and the first term on the right represents entrainment.

If $n_i = \rho_i/m$ is the number density where m_i is the molecular mass and $\dot{n}_i = \dot{\rho}_i/m_i$, then $dn_i/dt = (n_{ie} - n_i)/\tau_d + \dot{n}_i$ where $t = x/\bar{U}$ is a Lagrangian time scale (time since a fluid particle at x passed the origin or time at a fixed point once the vehicle has passed) and τ_d is a characteristic diffusion time,

$$\tau_d(t) = [(\bar{U}/A)(dA/dx)]^{-1} = (d\ln A/dt)^{-1}$$

For an elliptic wake, A is related to horizontal and vertical dispersion distances (σ_h and σ_v , respectively) by $A(t) = \pi\sigma_h(t)\sigma_v(t)$. Using dispersion distance in the literature for the postvortex wake (10^2 - 10^8 sec),² it can be demonstrated that $\tau_d \approx 0.55 t$. The chemical source term can now be rewritten as $\dot{n}_i(n_{ieq} - n_i)/\tau_{ic}$, where n_{ieq} is the local photochemical equilibrium concentration and τ_{ic} is the chemical reaction time. The functional dependence of n_{ieq} and τ_{ic} on other (n_j) concentrations can be derived by forming the appropriate photochemical production and loss terms.

If n_{iss} and τ_i are, respectively, the local steady-state concentration and effective time constant, $dn_i/dt = (n_{iss} - n_i)/\tau_i$ where $n_{iss} = (\tau_{ic}n_{ie} + \tau_d n_{ieq})/(\tau_{ic} + \tau_d)$ and $\tau_i = \tau_{ic}\tau_d/(\tau_{ic} + \tau_d)$. Assuming that n_{iss} and τ_i do not change too much across a time-step Δt (which may not always be the case)

$$n_i(\Delta t) = n_{iss}(0) + [n_i(0) - n_{iss}(0)]e^{-\Delta t/\tau_i(0)} \quad (2)$$

where (0) refers to the value of a quantity at the start of a time step. Equation (2) can be reduced to the pure chemistry result in Ref. (3) by assuming very slow diffusion ($\tau_d \rightarrow \infty$). Then, $\tau_i \rightarrow \tau_{ic}$ and $n_{iss} \rightarrow n_{ieq}$.

A truncated chemical reaction scheme⁴ utilizing O_3 , $O(^3P)$, NO , and NO_2 and five chemical reactions was used to debug the program. Unlike Ref. 3, utilization of a CDC 6600 computer allowed solution of Eq. (2), without maintaining the concentration of $[O(^3P)]$, at zero. The ratio $[NO]/[NO_2]$ obtained for pure chemistry is considerably smoother than the results in Fig. 1 of Ref. 4, where $[O(^3P)]$ was held at zero. A typical computer run solving Eq. (2) takes a small fraction of a minute.

A much more elaborate reaction scheme incorporates 44 photochemical reactions and the additional species N_2 , O_2 , $O(^1D)$, NO_3 , N_2O , N , HO_2 , HO , HNO_3 , H_2O_2 , H , CH_3 , and CH_3 .⁵ Chemical reaction rates are the most probable CIAP rates⁶ and the four sets of photolytic rates used are listed in Table 1.

Analysis and Conclusions

The first runs considered ozone depletion in pure chemistry wakes for comparison with results using the more cumbersome GEAR algorithm for the GE-4 engine.⁴ Variation of step size indicated close agreement for $\Delta t \leq 10$ sec out to $t = 1000$ sec. Errors in ozone depletion results are introduced

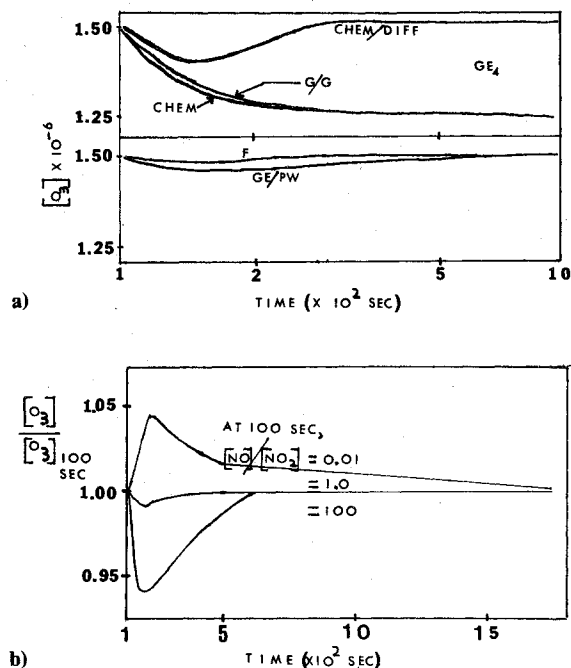


Fig. 1 Ozone depletion for GE4, Ferri, (F) and GE/PW Engines at 20 km vs time: a) For GE4, $\Delta t = 10$ sec, $\Delta t = 0.1t$ for other engines, G/G = Gupta and Grose's results and CHEM = pure chemistry, CHEM/DIFF = chemistry + diffusion; LLL photolysis; b) Effects of variation of 100 sec NO_x ratio upon ozone depletion for GE4 engine, LG photolysis; $\Delta t = 10$ sec, CHEM/DIFF.

for $\Delta t = 50$ - 150 sec, particularly in cases where $\Delta t \geq \tau_i$, where τ_i changes substantially over the time step. Also, for $\Delta t = 50$ - 150 sec, NO_x mass is not conserved, whereas it is to 1% out to $t = 1000$ sec for $\Delta t = 10$ sec.

Figure 1a compares chemistry/diffusion results, curves for pure chemistry and Gupta and Grose's (G/G) data.⁴ Ozone depletion curves in Fig. 1a are for three engines: The GE4,^{3,4} an advanced engine discussed by Ferri,³ and an intermediate GE/PW engine considered in clean combustor studies by the General Electric Co. and Pratt and Whitney Corp.⁸ Emission characteristics of these engines (NO_x , H_2O g effluent/kg fuel) are GE-4 (18.0, 1250) GE/PW (9.0, 1250) and Ferri (3.6, 1250). Although Fig. 1a is for LLL photolysis, the corresponding results for the other schemes are very similar.

In analyzing the data, it was found that insubstantial errors were introduced if initial wake and ambient H_2O concentrations were equal, at least during the first few thousand seconds of the postvortex period. From measurements, it is doubtful that an independent wake exists after a few thousand seconds.⁹ Ambient concentrations of H_2O and other species are listed in Refs. 10-12. It was also discovered

Table 1 Photolytic reaction rates utilized in this analysis (height = 20 km)

Reactions	LG ^b (sec ⁻¹)	LLL ^c (sec ⁻¹)	FL-S ^d (sec ⁻¹)	FL-N ^e (sec ⁻¹)
$O_2 \xrightarrow{h\nu} O + O$	1.50×10^{-15}	4.68×10^{-14}	7.60×10^{-14}	6.87×10^{-14}
$O_3 \xrightarrow{h\nu} O_2 + O(^3P)$	2.80×10^{-4}	2.09×10^{-4}	3.01×10^{-4}	2.08×10^{-4}
$O_3 \xrightarrow{h\nu} O_2 + O(^1D)$	0.50×10^{-5}	9.14×10^{-6}	1.24×10^{-5}	8.17×10^{-6}
$NO_2 \xrightarrow{h\nu} NO + O$	0.80×10^{-2}	4.74×10^{-3}	7.76×10^{-3}	4.74×10^{-3}
$N_2O \xrightarrow{h\nu} N_2 + O(^1D)$	8.68×10^{-11}	8.68×10^{-11}	1.36×10^{-10}	1.16×10^{-10}
$NO \xrightarrow{h\nu} N + O$	7.30×10^{-29}	7.30×10^{-29}	7.30×10^{-27}	7.30×10^{-27}
$HNO_3 \xrightarrow{h\nu} HO + NO_2$	3.57×10^{-7}	3.57×10^{-7}	5.23×10^{-7}	3.42×10^{-7}
$H_2O_2 \xrightarrow{h\nu} HO + HO$	2.39×10^{-6}	2.39×10^{-6}	3.49×10^{-6}	2.26×10^{-6}
$HO_2 \xrightarrow{h\nu} HO + O$	8.70×10^{-9}	8.70×10^{-9}	1.40×10^{-8}	1.26×10^{-8}
$NO_3 \xrightarrow{h\nu} NO_2 + O^a$	1.00×10^{-2}	1.00×10^{-2}	1.00×10^{-2}	1.00×10^{-2}

^a Calculated by assuming this reaction to be only fate of NO_3 . ^b Reference 7, 1/2 of 60° solar zenith angle photolytic rates for direct insolation and multiple backscatter (earth surface albedo: 0.25). ^c Supplied by H. W. Elsaesser, May 1976; no multiple scattering, 1/2 noon value of direct solar insolation, 45° sun. ^d Supplied by F. Luther, Jan. 17, 1976. Most recent Lawrence Livermore rates: 45° sun, 1/2 of solar constant, 0.25 earth surface albedo. ^e Same as FL-S except no multiple scattering.

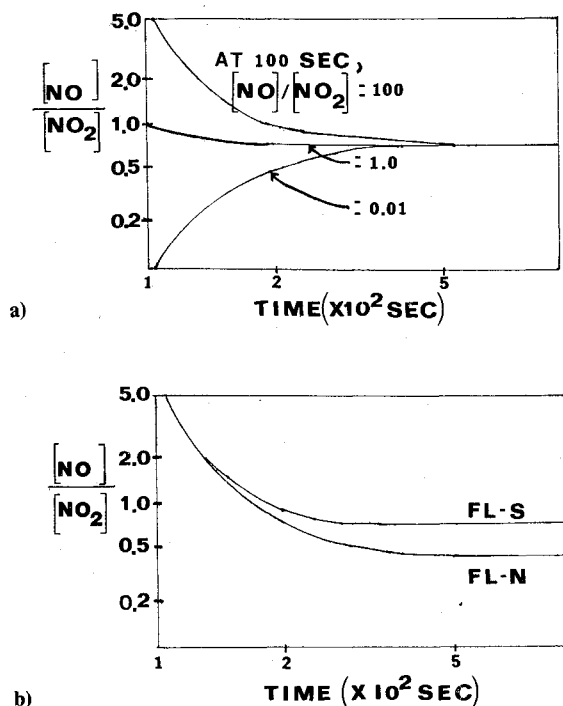


Fig. 2 NO_x ratio as a function of time and 100 sec NO_x ratio, for GE4 engine at 20 km and CHEM/DIFF. a) LG photolysis, $\Delta t = 10$ sec. b) FL-S and FL-N photolysis to demonstrate effect of multiple scattering, $\Delta t = 10$ sec.

that ozone depletion results in the early postvortex period are very similar for the truncated and complete reaction schemes.

Gupta and Grose considered ozone-depletion effects of variation in initial value of [NO]/[NO₂] in a pure chemical SST wake for the GE4 engine, using a 12-species, 20-reaction scheme. Figure 1b, calculated from Eq. (2), includes the effects of diffusion as well. Comparison with Gupta and Grose's Fig. 6 indicates that entrainment reduces the intensity and duration of the "ozone hole." As with pure chemistry, a chemistry/diffusion wake with a very low initial [NO]/[NO₂] can result in a slight increase in [O₃] within the early post-vortex period. It is most unlikely that this effect would result in a global increase in [O₃] by widespread SST operations, since engine NO_x production would be independent of initial [NO]/[NO₂]. The global catalytic ozone depletion effects of this NO_x will be much more significant than a small "negative ozone hole." It is also of interest to note that the initial [NO]/[NO₂] is only significant in the very near wake.

The photolysis schemes in Table 1 are much more significant than the initial [NO]/[NO₂] in determining inputs to a global model. Figure 2a presents this NO_x ratio as a function of time for a GE4 engine at 20 km using LG photolysis. Note that the photochemical equilibrium value of [NO]/[NO₂] = 0.69 is reached by 500 sec, regardless of the initial [NO]/[NO₂]. Qualitatively similar results were obtained using LLL photolysis, with a photochemical equilibrium value of [NO]/[NO₂] = 0.41. Other researchers have reported similar effects.¹³ From Table 1, to a very close approximation $\{[NO]/[NO_2]\}_{\text{photo.eq., LLL}} / \{[NO]/[NO_2]\}_{\text{photo.eq., LG}} \approx \{J_{NO_2}\}_{\text{LLL}} / \{J_{NO_2}\}_{\text{LG}}$, where J_{NO_2} is the photolysis rate for NO₂ → NO + O.

Reaction rates FL-S and FL-N in Table 1 are for the same sun angle, with and without consideration of earth albedo and multiple scattering. Figure 2b reveals that the photochemical equilibrium value of [NO]/[NO₂] for a 45° sun, GE4 at 20 km is 0.69 with scattering, 0.42 without scattering. The effects of omitting multiple scattering from an ozone depletion model's

photolysis rates would be considerable. The effluent output after several thousand seconds of the postvortex period is significant, because this will be the input to the global models discussed by Hidalgo and others.¹⁴ According to Hidalgo, the effluent index is usually given in terms of grams of NO₂ emitted per kilogram of fuel. In the unperturbed daytime stratosphere, [NO]/[NO₂] = 0.4-1.0 as a function of measurement height, sun altitude, time of day, and model.¹¹

This Note indicates that [NO]/[NO₂] in an SST wake at photochemical equilibrium is a strong function of photolysis rates. Because no more than a fraction of a minute is required to model the wake out to several thousand seconds using our photochemical scheme, we are currently preparing a simple one-dimensional model to investigate the effects of variation in wake photochemical equilibrium [NO]/[NO₂] upon global ozone depletion. Because of the computational speed of the technique, extensive sensitivity studies should be possible.

Acknowledgment

This research was supported by NASA Grant NSG-1298. The assistance of H. W. Ellsaesser and F. Luther is appreciated.

References

- Lin, S. C. and Hayes, J. E., "A Quasi-One-Dimensional Treatment of Chemical Reactions in Turbulent Wakes of Hypersonic Objects," *AIAA Journal*, Vol. 2, July 1964, pp. 1214-1222.
- Bauer, E., "Introduction and Overview: The Stratosphere and its Application to CIAP," and Danielsen, E., "Introduction: Transport by Mean and Turbulent Motions," *The Natural Stratosphere of 1974, CIAP Monograph 1*, DOT-TST-75-51 (A. J. Groebecker, editor), Dept. of Transportation, Washington, D.C., Sept. 1975, Chap. 1 and Sec. 6.1.
- Matloff, G. L., "Technique for Atmospheric Rate Chemistry Calculations," *AIAA Journal*, Vol. 14, July 1976, pp. 987-988.
- Gupta, R. N. and Grose, W., "Some Aspects of the Ozone-Depletion Problem in the Stratosphere," *AIAA Journal*, Vol. 13, June 1975, pp. 792-796.
- Duewer, W. H., Wuebbles, D. J., Ellsaesser, H. W., and Chang, J. S., "NO_x Catalytic Ozone Destruction: Sensitivity to Rate Coefficients," *Journal of Geophysical Research*, Vol. 82, Feb. 20, 1977, pp. 935-942.
- Johnston, H. S., et al., "Chemistry in the Stratosphere," *The Natural Stratosphere of 1974, CIAP Monograph 1*, DOT-TST-75-51, (A. J. Groebecker, editor), Dept. of Transportation, Washington, D. C., Sept. 1975, Chap. 5.
- Luther, F. M. and Gelinas, R. J., "Effect of Molecular Multiple Scattering and Surface Albedo on Atmospheric Photodissociation Rates," *Journal of Geophysical Research*, Vol. 81, Feb. 1976, pp. 1125-1132.
- Weber, R. J., "NASA Propulsion Research for Supersonic Cruise Aircraft," *Astronautics and Aeronautics*, Vol. 14, May 1976, pp. 38-45.
- Farlow, N. H., Watson, V. R., Loewenstein, M., Chan, K. L., Hoshizaki, H., Conti, R. J., and Meyer, J. W., "Measurements of Supersonic Jet Aircraft Wakes in the Stratosphere," presented at the Second International Conference on the Environmental Impact of Aerospace Operations in the High Stratosphere, Jan. 8-10, 1974, San Diego, Calif.
- Stewart, R. W. and Hoffert, M. I., "A Chemical Model of the Troposphere and Stratosphere," *Journal of Atmospheric Sciences*, Vol. 32, Jan. 1975, pp. 195-210.
- Shimazaki, T. and Whitten, B. C., "A Comparison of One-Dimensional Theoretical Models of Stratospheric Minor Constituents," *Reviews of Geophysics and Space Physics*, Vol. 14, Feb. 1976, pp. 1-12.
- Gelinas, R. J. and Walton, J. J., "Dynamic-Kinetic Evolution of a Single Plume of Interacting Species," *Journal of the Atmospheric Sciences*, Vol. 31, Oct. 1974, pp. 1807-1813.
- Nicolet, M., "Stratospheric Ozone: An Introduction to Its Study," *Reviews of Geophysics and Space Physics*, Vol. 12, No. 5, Nov. 1975, pp. 593-636.
- Hidalgo, H., "Assessment of Potential Impact of Stratospheric Flight on Earth's Ultraviolet Irradiance," *AIAA Journal*, Vol. 14, Feb. 1976, pp. 137-149.